

## MIT Open Access Articles

*Large area selective emitters/absorbers based on 2D tantalum photonic crystals for high-temperature energy applications*

The MIT Faculty has made this article openly available. **Please share** how this access benefits you. Your story matters.

**Citation:** Rinnerbauer, V., Y. X. Yeng, J. J. Senkevich, J. D. Joannopoulos, M. Soljačić, and I. Celanovic. "Large Area Selective Emitters/absorbers Based on 2D Tantalum Photonic Crystals for High-Temperature Energy Applications." Edited by Ali Adibi, Shawn-Yu Lin, and Axel Scherer. Photonic and Phononic Properties of Engineered Nanostructures III (February 21, 2013). (Proc. of SPIE; v. 8632). © [2013] SPIE.

**As Published:** <http://dx.doi.org/10.1117/12.2005202>

**Publisher:** Society of Photo-Optical Instrumentation Engineers (SPIE)

**Persistent URL:** <http://hdl.handle.net/1721.1/88486>

**Version:** Final published version: final published article, as it appeared in a journal, conference proceedings, or other formally published context

**Terms of Use:** Article is made available in accordance with the publisher's policy and may be subject to US copyright law. Please refer to the publisher's site for terms of use.



# Large area selective emitters/absorbers based on 2D tantalum photonic crystals for high-temperature energy applications

V. Rinnerbauer\*<sup>a</sup>, Y. X. Yeng<sup>a</sup>, J. J. Senkevich<sup>a</sup>, J. D. Joannopoulos<sup>a</sup>, M. Soljačić<sup>a</sup>, I. Celanovic<sup>a</sup>  
<sup>a</sup>Massachusetts Institute of Technology, Cambridge, MA, USA 02139

## ABSTRACT

We report highly selective emitters based on high-aspect ratio 2D photonic crystals (PhCs) fabricated on large area (2 inch diameter) polycrystalline tantalum substrates, suitable for high-temperature operation. As an example we present an optimized design for a selective emitter with a cut-off wavelength of 2 $\mu$ m, matched to the bandgap of an InGaAs PV cell, achieving a predicted spectral selectivity of 56.6% at 1200K. We present a fabrication route for these tantalum PhCs, based on standard microfabrication processes including deep reactive ion etch of tantalum by an SF<sub>6</sub> based Bosch process, achieving high-aspect ratio cavities (> 8:1). Interference lithography was used to facilitate large area fabrication, maintaining both fabrication precision and uniformity, with a cavity diameter variation of less than 2% across the substrate. The fabricated tantalum PhCs exhibit strong enhancement of the emittance at wavelengths below cut-off wavelength, approaching that of blackbody, and a steep cut-off between high and low emittance spectral regions. Moreover, detailed simulations and numerical modeling show excellent agreement with experimental results. In addition, we propose a surface protective coating, which acts as a thermal barrier coating and diffusion inhibitor, and its conformal fabrication by atomic layer deposition.

**Keywords:** photonic crystal, high-temperature, thermophotovoltaic, thermal emitter, tantalum

## 1. INTRODUCTION

Metallic two-dimensional photonics crystals (PhCs) are highly promising as high-performance selective thermal emitters and absorbers for solid-state high-temperature (>1000K) thermal-to-electrical energy conversion schemes including thermophotovoltaic (TPV), solar-thermophotovoltaic, solar-thermal and solar-thermochemical systems. After decades of intense studies focused on cryogenic and room temperature nanophotonics, scientific interest is also growing in high-temperature nanophotonics aimed at solid-state energy conversion. These latest extensive research efforts are spurred by a renewed interest in high temperature thermal-to-electrical energy conversion schemes including thermophotovoltaics (TPV), solar-thermophotovoltaics, solar-thermal, and solar-thermochemical energy conversion systems. Theoretical studies have shown that thermophotovoltaics has the potential for highly efficient thermal-to-electrical energy conversion, and even to surpass the Shockley-Queisser limit for single-junction PV cells, which is 41% efficiency under full concentration of sunlight and 31% without concentration<sup>1</sup>. In contrast solar TPV systems can have theoretical efficiencies of up to 54% without and 85% under full concentration of sunlight<sup>2,3</sup> which is very close to the theoretical limit for a tandem configuration of infinitely many PV cells with different bandgaps of 86.8%.<sup>4</sup> to achieve the predicted theoretical efficiencies, highly selective emitters and absorbers which can be operated at high temperatures are vital.

Efficient design of highly selective and highly efficient radiation sources and absorbers is facilitated by the ability to tailor the photonic density of states and thereby thermal radiation in PhCs. In the face of the targeted high operating temperatures (>1000 K) stringent challenges regarding material design have to be met, and proper material selection to prevent melting, evaporation or chemical reactions, severe minimization of any material interfaces to prevent thermochemical problems such as delamination and structural stability in the presence of surface diffusion are critical. For thermal stability and high performance at elevated temperatures it is most advantageous to use all-metallic 2D PhCs which reduces the number of interfaces.

\*vrinner@mit.edu; phone 1 617 324 6443; fax 1 617 253 5859

In particular, refractory metals exhibit low emissivity at long wavelengths and increasing emissivity in the near infrared, in addition to high melting points ( $> 3000$  K) and low vapor pressure. They also exhibit an intrinsic wavelength selective emissivity, showing low emissivity at wavelengths greater than  $\sim 2.5$   $\mu\text{m}$ . This low emissivity at long wavelengths is vital for selective emitters for energy conversion applications like TPV, since longer wavelength emission is generally below the bandgap of the current state of the art low bandgap TPV cells, and lost as waste heat. The increased emissivity below  $\sim 2.5$   $\mu\text{m}$  due to interband transitions on the other hand enables us to easily enhance emission in the wavelength range important for TPV energy conversion. This intrinsic wavelength selectivity is also necessary for application as an efficient solar selective absorber characterized by strong solar absorption and low thermal emissivity. In the past, studies on W PhC have demonstrated highly promising results regarding selective emitters and absorbers.<sup>5-10</sup>

In our recent approach we have investigated selective emitters based on tantalum (Ta), whose inherent material properties, such as its machinability and weldability, allow for simple integration of these devices into complex systems like high temperature solid state energy conversion schemes, bringing this highly promising field one step closer to high-efficiency applications. Our latest results of 2D Ta photonic crystals show a high level of spectral selectivity, enhancement of the emittance at wavelengths below cut-off wavelength approaching that of blackbody, and steep cut-off between high and low emissivity spectral regions. Moreover, detailed simulations show excellent agreement with experimental results. We have established a fabrication route to large area (2 inch, i.e. 5 cm diameter), high aspect ratio ( $> 8:1$ ) photonic crystals in polycrystalline tantalum, based on standard microfabrication processes. These exciting results enable scaling up the fabrication for large area, highly efficient high-temperature selective emitters and absorbers. These large scale high performance selective emitters, suitable for high temperature operation, open up the route to high efficiency solid-state thermal-to-electrical energy conversion based on high-temperature nanophotonics.

## 2. SELECTIVE THERMAL EMITTERS

Selective radiation sources and absorbers are a common problem in energy conversion schemes, in particular in direct heat-to-electricity conversion. TPV energy conversion was first proposed in 1960's.<sup>11,12</sup> It is a direct thermal to electric energy conversion scheme, whereby photons produced by a thermal emitter drive a suitable low-bandgap photovoltaic (PV) cell. This concept permits direct thermal to electrical energy conversion without any mechanical components and on small device scales, i. e. with high power densities, fundamentally limited only by Planck's blackbody law. In a photovoltaic system, the efficiency is limited due to the mismatch of the radiation spectrum and the spectral properties of the PV diode: Photons with energies below the bandgap do not contribute to the electrical current, and for each high energy photon, the energy in excess of the bandgap is dissipated as waste heat (phonons) and thus lost in the sense of power conversion. The efficiency of any TPV system therefore depends on the careful match of the emitter spectrum to the electronic bandgap and spectral properties of the PV material, and can be tremendously increased by the use of spectrally selective emitters. Thus high performance, high-temperature selective emitters and absorbers enable a novel solid state energy conversion schemes, including solar, radioisotope and combustion TPV as well as solar-thermochemical energy conversion, with the potential for providing high efficiency, scalable energy solutions.

TPV has proven to be an extremely versatile energy production and conversion concept, as it can be employed to convert energy of any thermal source into electrical energy. Thus, a variety of applications have been proposed, encompassing combustion TPV,<sup>13-15</sup> radioisotope TPV<sup>16</sup> as well as solar TPV,<sup>17</sup> solar thermal and solar chemical applications<sup>18</sup> with highly promising key figures such as efficiency, power density and output power. In comparison to conventional thermal to electrical energy conversion by mechanical engines, the TPV concept offers the advantage of versatility of the 'fuel', higher reliability and less maintenance requirements due to the absence of moving parts, and the potential for smaller form factors and higher power densities. Indeed a micro-TPV system with a 1  $\text{cm}^2$  microreactor operating at 850  $^\circ\text{C}$  and an output power of 150 mW has been proposed and demonstrated.<sup>13</sup> Radioisotope TPV applications are used with radioisotope fuel cells, and allow for a very robust and stable energy source for long-term operation (18–30 years) in extreme environments, therefore ideal for space applications but also for terrestrial energy supply where other energy sources are not available or stable long-term operations is needed. Another promising technology that can potentially beat the Shockley–Queisser limit<sup>1</sup> is solar TPV, where the expected efficiencies and key figures have been particularly well studied.<sup>2,19,20</sup> In the solar TPV system, (concentrated) solar radiation is absorbed by a selective absorber and used to heat a selective emitter. This combined absorber/emitter structure can be designed to efficiently absorb broadband solar radiation and convert it to suitable narrow-band emission matching the bandgap of the PV cell.

The necessary selectivity of absorption and (thermal) emission can be achieved by PhCs, since they offer supreme control the photonic density of states, and thereby also thermal emission and absorption. The photonic modes introduced by the cavities of a 2D metallic PhC allow the radiation to be more efficiently absorbed and emitted, reducing the intrinsic reflectivity of the flat metallic substrate. The emissivity in the wavelength range of these cavity modes is therefore enhanced up to the blackbody limit, with a steep cut-off wavelength that is determined by the fundamental mode of the cavity, as radiation with longer wavelengths is forbidden from entering the cavity. Thus the cut-off can be efficiently tailored by tailoring the diameter of the cavities of the PhC, and the emissivity above the cut-off wavelength is kept low.

In Figure 1 the simulated spectral emission of a Ta PhC at normal angle, optimized for a cut-off wavelength of  $\lambda_{PV}=2.0\mu\text{m}$  is compared to the emission of flat Ta<sup>21</sup> and blackbody emission at 1200 K. We employ a finite difference time domain (FDTD) algorithm<sup>22</sup> implemented via MEEP,<sup>23</sup> a freely available software package developed at MIT, for simulation of the optical properties of the PhCs, which are designed as a square array of circular cavities with a period  $a$ , radius  $r$  and cavity depth  $d$  etched into the substrate (see inset in Fig. 1). The optical dispersion relation of Ta is incorporated in the simulations via a Lorentz–Drude oscillator model, whose parameters are fitted to the experimentally measured reflectance of flat polished Ta. By matching the quality (Q) factors of the radiative and absorbing modes of the cavities of the PhC<sup>10,24</sup> the emission below the cutoff wavelength is greatly increased from the intrinsic emission of flat Ta, approaching that of a blackbody. At the same time, the emission at wavelengths above the cut-off is kept low, approaching that of the bare substrate for long wavelengths (above 6  $\mu\text{m}$ ), minimizing losses due to waste heat and achieving high selectivity. The optimized parameters of this PhC, designed for a cut-off wavelength of  $\lambda_{PV}=2.0\mu\text{m}$  are a cavity radius of  $r=0.54\mu\text{m}$ , a period  $a=1.3\mu\text{m}$  and an etch depth of  $d=8.0\mu\text{m}$ . With this design, a normal spectral efficiency (i.e. the ratio of useful emitted power below the cut-off wavelength to the total emitted power at a given temperature) of 56.6% can be achieved at 1200 K.

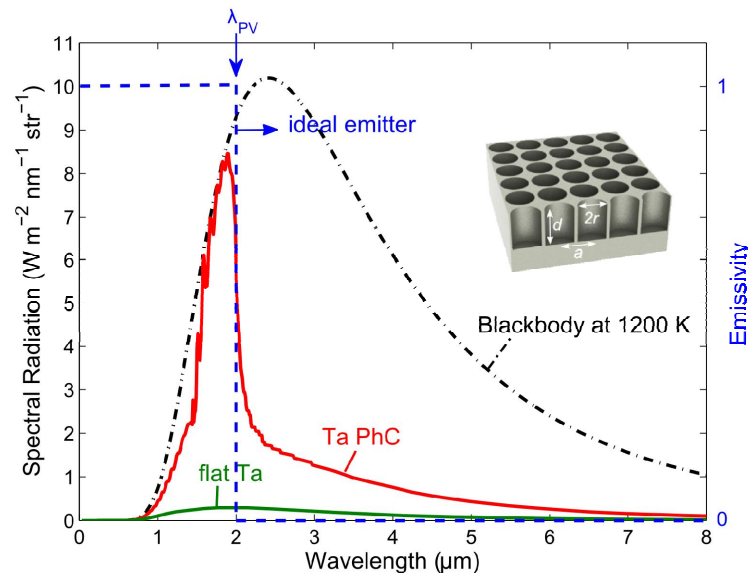


Fig. 1. Simulated normal spectral emission at 1200 K of a Ta PhC optimized for a cutoff wavelength of  $\lambda=2.0\mu\text{m}$  with radius  $r=0.54\mu\text{m}$ , a period  $a=1.3\mu\text{m}$  and an etch depth of  $d=8.0\mu\text{m}$  compared to that of flat Ta (solid lines) and that of a blackbody emitter (dashed-dotted line) at the same temperature, and the emissivity of an ideal emitter (dashed line). Inset: schematic view of the PhC.

### 3. FABRICATION

#### 3.1 Materials and substrate preparation

Substrates of 3/4 inch (1.9 cm) and 2 inch (5 cm) diameter, and 3 mm thickness made from high purity (>99.9%) polycrystalline Ta (Rembar) were used to fabricate 2D PhCs for selective emitters. Essential to the PhC fabrication is the flatness, small surface roughness, large grain size and high thermal stability of the Ta substrate. Polycrystalline Ta is more affordable and readily available in large-area substrates as opposed to single crystal substrates. On the other hand, polycrystalline metals typically have grain sizes that are smaller or comparable to the feature size of PhC and are much less thermally stable than single crystals. Small grain size is detrimental to the performance of high-temperature nanophotonic devices for two reasons: firstly, small grain size on the order of the PhC feature sizes could interfere with PhC pattern and lead to poor optical performance, and secondly, polycrystalline material is thermodynamically unstable at high temperatures, and hence grain boundary migration and grain growth could lead to disintegration of the PhC structure. Therefore, large grain size (>> feature size) substrates are critical as a starting point for high-temperature nanophotonics. We achieve this by pre-annealing of the polycrystalline substrates at high temperature.

To prepare substrates for nanofabrication, the polycrystalline substrates were cut, lapped and annealed at 2250°C under vacuum for 4h with a slow heating and cooling ramp. After annealing, the substrates showed a bifurcated grain structure with large grains on the order of 1-2 mm across and small grains of 0.1-0.5 mm across. The substrates were subsequently lapped and polished to an optical degree with a surface roughness of  $R_a < 1$  nm and a flatness and parallelism on the order of 2.5  $\mu\text{m}$  and 12.5  $\mu\text{m}$ , respectively.

#### 3.2 Photonic crystal fabrication

The fabrication of the PhCs involves the steps of pattern definition by interference lithography (IL) based on a trilayer resist process<sup>25</sup>, defining the final cavity diameter by ashing of the photoresist and antireflective coatings, pattern transfer to a thin chrome (Cr) hard mask by reactive ion etching (RIE), and the final etching of the substrate by deep reactive ion etching (DRIE) using an SF<sub>6</sub> based Bosch process. As we employ achromatic interference lithography on a Mach-Zehnder setup<sup>26</sup> the fabrication scheme is easily scalable to large area substrates while maintaining long range fabrication precision over large areas. IL is a relatively inexpensive, fast and precise maskless lithography method, which relies on the interference pattern generated by two coherent light sources to define 1D and 2D periodic patterns in a single plane, and is easily scalable to large exposure areas. The periodicity of the pattern is defined by the interference angle, and the exposure is performed twice, with the substrates rotated by 90° between exposures to create a square array of cylindrical cavities. Due to the distribution of the intensity in the plane of the substrate, the diameter of the non-exposed circular areas increases from the center to the edge of the exposed area, causing a slight variation of the cavity diameter. We established a SF<sub>6</sub>/C<sub>4</sub>F<sub>8</sub> based Bosch process to etch the Ta, using an Alcatel AMS100 DRIE. The process parameters of this step were optimized for deep cavities in Ta and maximum sidewall straightness, using the following values: SF<sub>6</sub> (200 sccm) / C<sub>4</sub>F<sub>8</sub> (100 sccm) with 3s/1.5s pulses, respectively, power 1200 W, pressure ~3 mT, substrate bias 75 W and temperature 20°C. For these process parameters, we achieve an etch rate of approximately 14 nm/s for Ta. The pulse duration of the etch step (SF<sub>6</sub>) and passivation step (C<sub>4</sub>F<sub>8</sub>) was optimized to 3:1.5 to achieve complete passivation of the sidewalls. To achieve straight sidewalls, it is imperative to keep the substrate temperature low, therefore repeated short etch steps of maximum 5 min duration were used. With this process we have been able to achieve up to 8.5  $\mu\text{m}$  deep cavities with an aspect ratio of up to 8, very steep sidewalls and negligible sidewall roughness, and very good etch selectivity. The selectivity of the Ta etch step is high enough that a layer of 50 nm of Cr is sufficient to achieve this etch depth, with the Cr layer thickness hardly reduced by the etch, so the selectivity amounts to at least 200.

Figure 2 shows scanning electron micrographs of the Ta PhC at different fabrication steps: the cavities in the exposed and developed photoresist after IL (Fig. 2a) have a diameter of less than half the period, therefore the diameter has to be enlarged by plasma ashing the antireflection coating (ARC) to the desired value (Fig. 2b); subsequently, the Cr hard mask is etched by RIE (Fig. 2c) and finally the Ta is etched by DRIE (Fig. 2d). The etch depth obtained on different samples is approximately 6-8.5  $\mu\text{m}$ , as estimated from SEM images of the cross section at a defect site, as the sample cannot be cleaved or cut easily, and the etch depth of the cavities is too high for AFM measurements. The fabricated samples show remarkable fabrication accuracy and uniformity across the sample area.

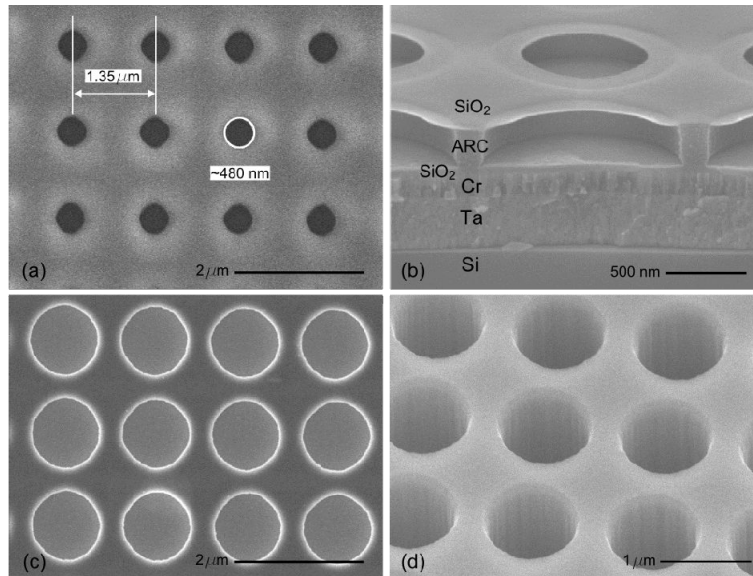


Figure 2. Scanning electron micrographs of the Ta during the fabrication steps: (a) developed photoresist after IL, (b) ashing of the antireflection coating to achieve target cavity diameter (cross-section from control sample on Si substrate), (c) Cr hard mask etched by RIE, (d) cavities etched into Ta by DRIE, with remaining Cr mask on top.

After etching of the cavities and removal of the Cr mask, a thin layer of  $\text{HfO}_2$  (20 nm) is deposited by atomic layer deposition (ALD) which ensures completely conformal deposition even in the high-aspect ratio cavities. The  $\text{HfO}_2$  layer does not influence the optical properties of the PhCs, save for a slight shift ( $\sim 40$  nm) of the cut-off wavelength to longer wavelengths as expected.

## 4. RESULTS AND DISCUSSION

### 4.1 Emissivity

As an example, we designed and fabricated a Ta PhC for a cut-off wavelength of  $\lambda_{\text{PV}}=2.0$   $\mu\text{m}$  (corresponding to a bandgap of 0.62 eV). The parameters of the PhC were optimized to achieve a spectral emissivity approaching an ideal step-function with this cut-off wavelength, resulting in an optimized cavity radius  $r=0.54$   $\mu\text{m}$ , a period  $a=1.3$   $\mu\text{m}$  and an etch depth  $d=8.0$   $\mu\text{m}$ , see above. As the emissivity of bare Ta below this cut-off wavelength is low, the PhC needs deep cavities to achieve a high quality factor  $Q$  of the fundamental cavity resonant mode, and a long interaction time of the radiation in this mode to be efficiently absorbed, to achieve a strong increase in emissivity. To facilitate fabrication, the etch depth of the cavities was limited to 8  $\mu\text{m}$  in the optimization. Simulations have shown that for increased cavity depth above  $\sim d=8.0$   $\mu\text{m}$ , the benefit of increased selectivity of the emissivity further is diminishing. A sharp cut-off between the high emissivity range approaching unity and the low emissivity range, limited by the intrinsic emissivity of Ta, can be achieved even for this etch depth.

The spectral emissivity of fabricated Ta PhCs is obtained from near normal incidence reflectivity measurements at room temperature. As the samples are opaque, transmission is zero and according to Kirchhoff's law the emissivity  $E$  and the reflectivity  $R$  amount to unity for every wavelength, therefore  $E = 1 - R$ . The measured emissivity of a Ta PhC fabricated on a 2 inch diameter substrate is shown in Figure 3, and a digital photo of the full 2 inch PhC is shown in the inset. As can be seen, there is a substantial increase of the emissivity below the cut-off at 2  $\mu\text{m}$  as compared to that of flat Ta, while the emissivity above the cut-off is kept low. A sharp cut-off between high and low emissivity regions is achieved, offering a 4:1 emissivity contrast over a wavelength range of 10%. The measured emissivity shows remarkable agreement with simulated results as shown in Figure 3, where the parameters  $r=0.53$   $\mu\text{m}$ ,  $a=1.33$   $\mu\text{m}$  and  $h=6.18$   $\mu\text{m}$  were used for simulation by FDTD. As discussed, there is a variation of the cavity diameter that is intrinsic to the use of IL on

large-area substrates. This variation results in  $\sim 20$  nm or  $\Delta 2r = 1.9\%$  increase of the diameter of the final cavities from the center to the edge of the 2 inch substrate. Correspondingly, the cut-off wavelength shifts by  $\sim 40$  nm or  $\Delta\lambda = 2\%$  to longer wavelengths when measured in the center or on the edge of the substrate (see inset of Fig. 3). We also demonstrated the fabrication of the PhC in the Cr hard mask on a 4 inch Si wafer using the same process. In this case, the variation of the cavity diameter was  $\sim 80$  nm or  $\Delta 2r = 7\%$  from the center to the edge of the 4 inch wafer.

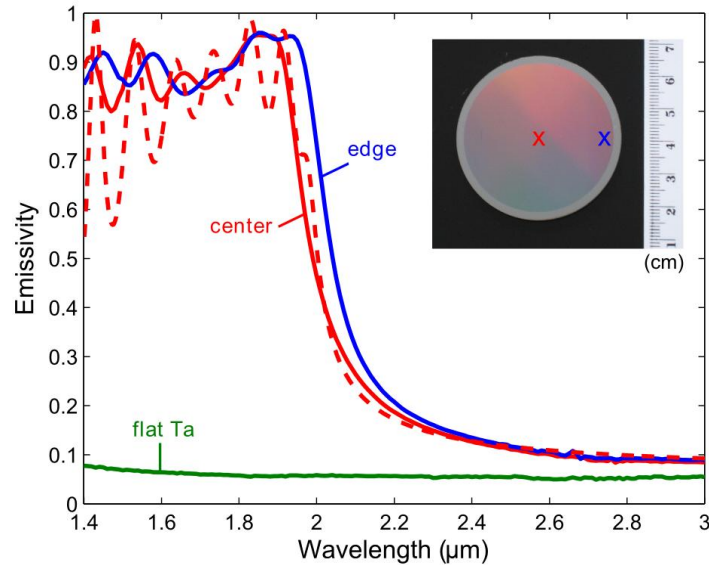


Figure 3. Measured room temperature emissivity of fabricated Ta PhC on 2 inch substrate measured in the center and towards the edge of the sample (solid lines) as compared to simulation (dashed line) with  $r=0.53\mu\text{m}$ ,  $a=1.33\mu\text{m}$  and  $h=6.18\mu\text{m}$ , and measured emissivity of flat Ta. Inset: Digital photo of the full 2 inch diameter sample after etching of the Cr hard mask; crosses indicate approximate measurement positions.

## 4.2 Thermal stability

As the target applications in energy conversion typically require operating temperatures  $\geq 1200$  K, there are stringent requirements on the thermal stability of all components involved. The thermal stability of nanostructured surfaces has been studied in few works<sup>27-29</sup>. In these studies, it was reported that there is the risk of complete disintegration of the nanostructure, especially on polycrystalline materials, even after short times (1 hour) at elevated temperatures. As reported, the structural deterioration is partly due to surface diffusion and partly due to recrystallization and grain migration. We used preannealed substrates, leading to large, stable grains, to approach the latter two problems and increase the thermal stability of the nanostructures by providing a thermally stable substrate. In addition, we use a thin conformal layer of  $\text{HfO}_2$  on top of our PhC for increased thermal stability. We expect this protective layer to reduce surface diffusion and surface reactions with surface contaminants or other contaminants, especially carbon, from non-ideal vacuum conditions under high-temperature operation. In some studies of nanostructured refractory metals,  $\text{HfO}_2$  was used before to increase the thermal stability.<sup>28,30</sup>

Preliminary experimental results demonstrate the high-temperature stability of the PhC structures and their emissivity for  $> 1$  h at  $1000^\circ\text{C}$  without any performance or structural degradation. In addition we have performed multiple longer time scale annealing tests at  $900^\circ\text{C}$  without degradation of the optical properties, showing that this is a promising route to thermal stability of nanostructured selective thermal emitters. Further evaluation of the long-term stability and high-temperature emission is under way.

## CONCLUSION

We have demonstrated highly selective emitters based on 2D Ta PhCs, suitable for high-temperature applications e. g. in energy conversion. We have established a fabrication route for large-area, high aspect ratio photonic crystals achieving outstanding fabrication uniformity and accuracy across samples of 2 inch diameter. High-purity polycrystalline Ta substrates were used as a starting point and annealed at high temperatures to achieve large grains and minimize grain boundary diffusion at high temperatures, then lapped and polished to an optical degree. PhCs comprising a square array of cylindrical cavities were fabricated on these polycrystalline Ta wafers of up to 2 inch diameter, using interference lithography and reactive ion etching techniques. We have developed a deep reactive ion etch process for Ta using an  $\text{SF}_6/\text{C}_4\text{F}_8$  based Bosch process, that enabled us to achieve up to 8.5  $\mu\text{m}$  deep cavities with an aspect ratio of up to 8, with very steep sidewalls and outstanding selectivity of the etch towards the Cr hard etch mask. The fabrication of the Cr hard mask was optimized using RIE to achieve smooth sidewalls and eliminate random sidewall roughness as obtained from a chemical wet etch of Cr. The selective emitters fabricated by this method showed excellent spectral selectivity, enhancement of the emissivity below cut-off approaching unity and a sharp cut-off between the high emissivity region and the low emissivity region, while maintaining the low intrinsic emissivity of bare Ta above the cut-off wavelength. Moreover, the experimental results show excellent agreement with numerical simulations. A thin conformal layer of  $\text{HfO}_2$  is used as a surface protective coating to increase thermal stability of the nanostructured surface. Preliminary results show the structural and optical stability of the fabricated PhCs for >48h at 900°C and >1h at 1000°C.

These promising results demonstrate the efficiency and performance of selective emitters and absorbers based on 2D Ta PhCs. This work is leading the way to scale up high-temperature nanophotonic devices, facilitating cost-effective large-area, high performance applications in high-temperature solid-state energy conversion.

## ACKNOWLEDGEMENTS

The authors would like to thank Walker R. Chan for valuable discussions, Richard Kaszeta and Chris Munro (Creare) for support regarding substrate preparation, Robert D. Geil (University of North Carolina) for DRIE of Ta, James Daley at NSL (MIT) for film deposition, and Tim Savas for assistance and training in interference lithography. Fabrication of Ta PhCs was done in part at the Nanostructures Laboratory (NSL) at MIT and at the Center for Nanoscale Systems (CNS) at Harvard University, a member of the National Nanotechnology Infrastructure Network (NNIN), which is supported by the National Science Foundation under NSF award No. ECS-0335765. This work was partially supported by the Army Research Office through the Institute for Soldier Nanotechnologies under Contract Nos. DAAD-19-02-D0002 and W911NF-07-D000. Y. X. Y. and M. S. were partially supported by the MIT S3TEC Energy Research Frontier Center of the Department of Energy under Grant No. DE-SC0001299. V. R. gratefully acknowledges funding by the Austrian Science Fund (FWF): J3161-N20.

## REFERENCES

- [1] Shockley, W. and Queisser, H. J., "Detailed balance limit of efficiency of p-n junction solar cells", *J. Appl. Phys.* 32, 510 (1961).
- [2] Harder, N. and Würfel, H. P., "Theoretical limits of thermophotovoltaic solar energy conversion", *Semicond. Sci. Technol.* 18, S151 (2003).
- [3] DeVos, A., [Endoreversible Thermodynamics of Solar Energy Conversion], Oxford University Press (1992).
- [4] DeVos, A., "Detailed balance limit of the efficiency of tandem solar cells", *Journal of Physics D*, 13, 839 (1980).
- [5] Heinzl, A., Boerner, V., Gombert, A., Bläsi, B., Wittwer, V. and Luther, J., "Radiation filters and emitters for the NIR based on periodically structured metal surfaces", *J. Mod. Opt.* 47, 2399 (2000).
- [6] Sai, H. and Yugami, H. "Thermophotovoltaic generation with selective radiators based on tungsten surface gratings", *Appl. Phys. Lett.* 85, 3399 (2004).
- [7] Rephaeli, E. and Fan, S., "Tungsten black absorber for solar light with wide angular operation range", *Appl. Phys. Lett.* 92, 211107 (2008).
- [8] Celanovic, I., Jovanovic, N. and Kassakian, J., "Two-dimensional tungsten photonic crystals as selective thermal emitters", *Appl. Phys. Lett.* 92, 193101 (2008).



- [9] Araghchini, M., Yeng, Y. X., Jovanovic, N., Bermel, P., Kolodziejski, L. A., Soljagic, M., Celanovic, I. and Joannopoulos, J. D., "Fabrication of two-dimensional tungsten photonic crystals for high-temperature applications", *J. Vac. Sci. Technol. B* 29, 061402 (2011).
- [10] Yeng, Y. X., Ghebrehan, M., Bermel, P., Chan, W. R., Joannopoulos, J. D., Soljagic, M. and Celanovic, I. "Enabling high-temperature nanophotonics for energy applications", *PNAS* 109, 2280 (2012).
- [11] Kolm, H., "Solar-Battery Power Source", MIT-Lincoln Laboratory, Quarterly Progress Report, Solid State Research, Group 35 (1956).
- [12] Wedlock, B., "Thermo-photo-voltaic conversion", *Proc. IEEE* 51, 694–698 (1963).
- [13] Pilawa-Podgurski, R. C. N., Pallo, N. A., Chan, W. R., Perreault D. J. and Celanovic, I. L., "Low-power maximum power point tracker with digital control for thermophotovoltaic generators", *Applied Power Electronics Conference and Exposition (APEC), Twenty-Fifth Annual IEEE*, pp.961–967 (2010).
- [14] Zenker, M., Heinzl, A., Stollwerck, G., Ferber J., and Luther, J., "Efficiency and power density potential of combustion-driven thermophotovoltaic systems using GaSb photovoltaic cells", *IEEE Trans. Electron Devices*, 48, 367–376 (2001).
- [15] Wenming, Y., Siawkiang, C., Chang, S., Hong, X. and Zhiwang, L., "Research on micro-thermophotovoltaic power generators with different emitting materials", *J. Micromech. Microeng.* 15, S239 (2005).
- [16] Crowley, C. J., Elkouh, N. A., Murray S., and Chubb, D. L., "Thermophotovoltaic converter performance for radioisotope power systems", *AIP Conf. Proc.*, 746, 601–614 (2005).
- [17] Andreev, V. M., Vlasov, A. S., Khvostikov, V. P., Khvostikova, O. A., Gazaryan, P. Y., Sorokina, S. V. and Sadchikov, N. A., "Solar thermophotovoltaic converters based on tungsten emitters", *J. Sol. Energy Eng.* 129, 298–303 (2007).
- [18] A. Steinfeld, "Solar thermochemical production of hydrogen - a review", *Sol. Energy.*, 78, 603–615 (2005).
- [19] Spirkel, W. and Ries, H., "Solar thermophotovoltaics: An assessment", *J. Appl. Phys.*, 57, 4409(1985).
- [20] Davies, P. A. and Luque, A., "Solar thermophotovoltaics: brief review and a new look", *Sol. Energy Mater. Sol. Cells* 33,11–22 (1994).
- [21] E. D. Palik, [Handbook of Optical Constants of Solids], Elsevier, vol. 2, pp. 408–420 (1998).
- [22] Taflove, A. and Hagness, S. C., [Computational Electrodynamics: The Finite-Difference Time-Domain Method], Artech House, Boston (2000).
- [23] Oskooi, A. F., Roundy, D., Ibanescu, M., Bermel, P., Joannopoulos, J. D. and Johnson, S. G., "Meep: A flexible free-software package for electromagnetic simulations by the FDTD method", *Comput. Phys. Commun.* 181, 687–702 (2010).
- [24] Ghebrehan, M., Bermel, P., Yeng, Y. X., Celanovic, I., Soljagic, M. and Joannopoulos, J. D., "Tailoring thermal emission via Q-matching of photonic crystal resonances", *Phys. Rev. A*, 83, 033810 (2011).
- [25] Schattenburg, M. L., Aucoin, R. J. and R. C. Fleming, "Optically matched trilevel resist process for nanostructure fabrication", *J. Vac. Sci. Technol. B* 13, 3007 (1995).
- [26] Schattenburg, M. L., Anderson, E. H. and Smith, H. I., "X-ray/VUV transmission gratings for astrophysical and laboratory applications", *Physica Scripta* 41, 13 (1990).
- [27] Sai, H., Kanamori, Y. and Yugami, H., "High-temperature resistive surface grating for spectral control of thermal radiation", *Appl. Phys. Lett.* 82, 1685 (2003).
- [28] Arpin, K. A., Losego, M. D. and Braun, P., "Electrodeposited 3D tungsten photonic crystal with enhanced thermal stability", *Chem. Mater.* 23, 4783–4788 (2011).
- [29] Schlemmer, C., Aschaber, J., Boerner, V. and Luther, J., "Thermal stability of micro-structured selective tungsten emitters", *AIP Conf. Proc.* 653, 164 (2003).
- [30] Nagpal, P., Josephson, D. P., Denny, N. R., DeWilde, J., Norris, D. J. and Stein, A., "Fabrication of carbon/refractory metal nanocomposites as thermally stable metallic photonic crystals", *J. Mater. Chem.* 21, 10836–10843 (2011).